

OPTIMIZATION OF AN AXIALLY COMPRESSED RING AND STRINGER STIFFENED CYLINDRICAL SHELL WITH A GENERAL BUCKLING MODAL IMPERFECTION

David Bushnell, Fellow, AIAA, Retired, 775 Northampton Drive, Palo Alto, CA 94303

(This is an abridged version. See the full-length paper for more: panda2.papers/2007.axialcomp.pdf)

7.0 TWO MAJOR EFFECTS OF A GENERAL BUCKLING MODAL IMPERFECTION

Much of the following appears in Section 11.1 on p. 19 of [1K]. It is repeated here because this section is especially important. It briefly describes the behavior of a **stiffened cylindrical shell** with a **general buckling modal imperfection shape**. This behavior plays a major role in the evolution of the design during optimization cycles in PANDA2. Here it is assumed that the shortest wavelength of the general buckling modal imperfection is greater than the greatest stiffener spacing, as holds in Figs. 1 and 2, for example (disregarding the component of stringer bending-torsional deformation displayed in the expanded insert in Fig. 1a).

A general buckling modal imperfection in a **stiffened shell** has **two major effects**:

1. The imperfect stiffened panel or shell bends as soon as any loading is applied. This **prebuckling bending** causes significant **redistribution of stresses** between the panel skin and the various stiffener parts, thus affecting significantly many local and inter-ring buckling and stress constraints (margins).
2. The "**effective**" **circumferential curvature** of an imperfect cylindrical panel or shell depends on the amplitude of the initial imperfection, on the circumferential wavelength of the critical buckling mode of the perfect and of the imperfect shell, and on the amount that the initial imperfection grows as the loading increases from zero to the design load. **The "effective" circumferential radius of curvature of the imperfect and loaded cylindrical shell is larger than its nominal radius of curvature** because the larger "effective" radius corresponds to the maximum local radius of the cylindrical shell with a typical **inward circumferential lobe** of the initial and subsequently load- amplified buckling modal imperfection. In PANDA2 this larger local "effective" radius of curvature is assumed to be the governing UNIFORM radius in the buckling equations pertaining to the imperfect shell. For the purpose of computing the general buckling load, the imperfect shell is replaced by a new perfect cylindrical shell with the larger "effective" circumferential radius. By means of this device a complicated nonlinear collapse analysis is converted into a simple **approximate** bifurcation buckling problem - a linear eigenvalue problem. For each type of buckling modal imperfection (general, inter-ring, local [1E]) PANDA2 computes a "knockdown" factor based on the ratio:

(buckling load factor: panel with its "effective" circumferential radius)/ (7.1) (buckling load factor: panel with its nominal circumferential radius)

Figures 1a,b,c show a STAGS model of a typical general buckling modal imperfection shape (amplitude exaggerated) for an optimized "compound" model [1K] of an axially compressed cylindrical shell with external stringers and internal rings (Case 4 in Table 4 in this paper). In this compound model a 45-degree sector has both external stringers and internal rings modeled as branched shell units. A 315-degree sector, the remainder of the cylindrical shell, has smeared stringers and internal rings modeled as branched shell units. Figure 2 shows the deformed state of the imperfect compound model as loaded by the design load, $N_x = -3000$ lb/in axial

compression (STAGS load factor PA is close to 1.0). One observes three characteristics:

1. The stresses in the imperfect axially compressed shell have been redistributed as the globally imperfect shell bends under the applied axial compression. The maximum effective (von Mises) stress in this case, $s_{bar}(max) = 66.87$ ksi, occurs in the outstanding stringer flanges where the prebuckling deformation pattern of the imperfect shell has a maximum inward lobe.
2. The typical maximum "effective" circumferential radius also occurs where the deformation pattern has a maximum inward lobe. This larger-than-nominal circumferential radius is highlighted most clearly by the in-plane circumferential deformation of the interior ring located one ring spacing in from the right-hand curved edge of the STAGS model shown in Fig. 2. See the right-most expanded insert in Fig. 2.
3. There is an important phenomenon that occurs when **imperfect** cylindrical shells are **optimized**. This phenomenon has been described in previous papers [1K]. It occurs in the case of a stiffened cylindrical shell with an **imperfection in the form of the critical general buckling mode of the perfect shell. The optimum design of an imperfect stiffened cylindrical shell has a general buckling load factor that is usually considerably higher than load factors that correspond to various kinds of local and "semi-local" buckling, such as local buckling of the panel skin and stiffener segments, rolling of the stiffeners, and inter-ring buckling.** The general buckling margin of such a shell is usually not critical (near zero). In contrast, when a **perfect** stiffened cylindrical shell is optimized the general buckling load factor is usually very close to at least one local buckling load factor and is usually lower than many other local and "semi-local" buckling load factors. The general buckling margin of an optimized **perfect** shell is usually critical (near zero).

The cases explored in this paper exhibit this characteristic. Take, for example, the optimum designs called Case 1 and Case 2 in Table 4. In Case 1 a **perfect** shell is optimized. The margins for the Case 1 optimum design are listed in Table 10. Several of the margins for local and "semi-local" buckling are essentially equal to or greater than that for general buckling, and the general buckling margin is near zero (critical). In Case 2 a shell with a general buckling modal imperfection is optimized. The margins for the imperfect optimized shell are listed in Table 6 and those for the same optimum configuration but with the amplitude of the general buckling modal imperfection set equal to zero are listed in Table 7. In both Tables 6 and 7 the margin for general buckling is considerably higher than many of the margins corresponding to local and "semi-local" buckling. The general buckling margin of the optimized **imperfect** shell is well above zero (not critical).

Why does this happen? **The general buckling margin of optimized IMPERFECT stiffened shells is forced higher during optimization cycles because PREBUCKLING BENDING OF THE IMPERFECT SHELL increases with applied load approximately hyperbolically as the applied load approaches the general buckling load of the imperfect shell [1E]. If the general buckling load of the optimized imperfect shell were close to the design load, that is, if the general buckling margin were near zero (almost critical), there would be so much prebuckling bending near the design load that LOCAL STRESS AND BUCKLING MARGINS FOR THE STIFFENER PARTS AND FOR THE PANEL SKIN WOULD BECOME NEGATIVE BECAUSE THESE PARTS OF THE STRUCTURE WOULD BECOME HIGHLY STRESSED.**

19.0 REFERENCES

[1] Bushnell, D., et al, (A) "PANDA2 - Program for minimum weight design of stiffened, composite, locally buckled panels", Computers and Structures, Vol. 25 (1987) pp. 469-605. See also: (B) "Theoretical basis of the PANDA computer program for preliminary design of stiffened panels under combined in-plane loads", Computers and Structures, v. 27, No. 4, pp 541-563, 1987; (C) "Optimization of composite, stiffened, imperfect panels under combined loads for service in the postbuckling regime", Computer Methods in Applied Mechanics and Engineering, Vol. 103, pp 43-114, 1993; (D) "Recent enhancements to PANDA2" 37th AIAA Structures,

Dynamics, and Materials (SDM) Conference, April 1996; **(E)** "Approximate method for the optimum design of ring and stringer stiffened cylindrical panels and shells with local, inter-ring, and general buckling modal imperfections", Computers and Structures, Vol. 59, No. 3, 489-527, 1996, with W. D. Bushnell; **(F)** "Optimum design via PANDA2 of composite sandwich panels with honeycomb or foam cores", AIAA Paper 97-1142, AIAA 38th SDM Conference, April 1997; **(G)** "Additional buckling solutions in PANDA2", AIAA 40th SDM Conference, p 302-345, April 1999, with H. Jiang and N. F. Knight, Jr.; **(H)** "Minimum-weight design of a stiffened panel via PANDA2 and evaluation of the optimized panel via STAGS", Computers and Structures, Vol. 50, 569-602 (1994); **(I)** "Optimization of perfect and imperfect ring and stringer stiffened cylindrical shells with PANDA2 and evaluation of the optimum designs with STAGS", AIAA Paper 2002-1408, pp 1562-1613, Proceedings of the 43rd AIAA SDM Meeting, April, 2002, with C. Rankin; **(J)** "Optimum design of stiffened panels with substiffeners, AIAA Paper 2005-1932, AIAA 46th SDM Conference, April 2005, with C. Rankin; **(K)** "Difficulties in optimization of imperfect stiffened cylindrical shells, AIAA Paper 2006-1943, AIAA 47th SDM Conference, April 2006, with C. Rankin; **(L)**.../panda2/doc/panda2.news, a continually updated file distributed with PANDA2 that contains a log of all significant modifications to PANDA2 from 1987 on.

[18] Almroth, B. O. and Brogan, F. A., "The STAGS computer code", NASA CR-2950, NASA Langley Research Center, Hampton, VA, 1978.

[19] STAGS Brochure (2002) available online by request: crankin@rhombuscgi.com (pdf format).

[20] **(A)** Rankin, C.C., Stehlin, P., and Brogan, F.A., "Enhancements to the STAGS computer code", NASA CR-4000, NASA Langley Research center, Hampton, VA, 1986. See also: **(B)** Rankin, C.C., "Application of Linear Finite Elements to Finite Strain Using Corotation." AIAA Paper AIAA-2006-1751, 47th AIAA Structures, Structural Dynamics and Materials Conference, May 2006; **(C)** Rankin, C.C., Brogan, F.A., Loden, W.A., Cabiness, H.D., "STAGS User Manual – Version 5.0," Rhombus Consultants Group, Inc., Palo Alto, CA, Revised January 2005 (on-line). Previously Report No. LMSC P032594, Lockheed Martin Missiles and Space Company, Palo Alto, CA, June 1998; **(D)** Rankin, C.C., "The use of shell elements for the analysis of large strain response, AIAA Paper 2007-2384, 48th AIAA Structures, Structural Dynamics and Materials Conference, Hawaii, April 2007.

[21] Riks, E., Rankin C. C., Brogan F. A., "On the solution of mode jumping phenomena in thin walled shell structures", First ASCE/ASM/SES Mechanics Conference, Charlottesville, VA, June 6-9, 1993, in: Computer Methods in Applied Mechanics and Engineering, Vol. 136, 1996.

Table 1 Geometry, material properties, and loading of the stiffened cylindrical shell. (PANDA2 names for dimensions such as H(STR), B(STR), etc., are defined in Table 2). (From: AIAA 48th Structures, Structural Dynamics, and Materials Conference, Paper no. AIAA-2007-2216, 2007)

Geometry (cylindrical shell):

Length = 75 inches
Radius = 25 inches
External T-shaped major stringers
Internal T-shaped major rings

Material properties (aluminum):

Young's modulus = 10 msi
Poisson ratio = 0.3
Maximum allowable effective (von Mises) stress = \bar{s} (allowable) = 60 ksi; Stress constraints are active.
The material remains **elastic** in all the models explored in this paper. The effect of elastic-plastic material behavior is also determined for four of the STAGS models. (See the stress-strain curve is given in Fig. 81.)

Loading used for all cases except one:

-3000.0\$ Axial Resultant (lb/in), $N_x(1)$ Load Set A (The axial resultant $N_x = -6000$ lb/in in Case 6)
-0.1 \$ Hoop Resultant (lb/in), $N_y(1)$ Load Set A
0.0 \$ In-plane shear (lb/in), $N_{xy}(1)$ Load Set A
-0.004 \$ Uniform pressure, (psi), $p(1)$ Load Set A
Zero loading in Load Set B

Boundary conditions:

Simple support, but free to expand radially in the prebuckling phase.

Imperfection:

General buckling modal imperfection amplitude, $W_{imp} = +0.25$ inch and -0.25 inch.

Imperfect shells have two load cases:

Load Set 1: $W_{imp} = +0.25$ inch
Load Set 2: $W_{imp} = -0.25$ inch

User-specified axial halfwavelength of the initial general buckling modal imperfection equals 75 inches.

In several of the cases PANDA2 is permitted to change the imperfection amplitude, W_{imp} , as described in the text.

NOTE:

In PANDA2 the complete cylindrical shell is modeled as a panel that spans 180 degrees. In the absence of in-plane shear loading (torque, N_{xy}) and anisotropy the behavior of the 180-degree panel simply supported along its two straight edges is identical to that of a complete cylindrical shell. The optimum weights listed in Table 4 are the weights of half (180 degrees) of the cylindrical shells.

Margins corresponding to inequality constraints (see next table for definitions of variables, $V(i)$, $i = 1, 13$):

1. $-V(3)^{+1} + 20.V(6)^{-1} - 1$. (stringer web height, $H(STR)$, is less than 20 x stringer web thickness, $T(2)(STR)$)
1. $-V(4)^{+1} + 20.V(7)^{-1} - 1$. (stringer flange width, $W(STR)$, is less than 20 x stringer flange thickness, $T(3)(STR)$)
1. $-V(10)^{+1} + 20.V(12)^{-1} - 1$. (ring web height, $H(RNG)$, is less than 20 x ring web thickness, $T(4)(RNG)$)
1. $-V(11)^{+1} + 20.V(13)^{-1} - 1$. (ring flange width, $W(RNG)$, is less than 20 x ring flange thickness, $T(5)(RNG)$)
1. $+V(8)^{+1} - V(11)^{-1} - 1$. (ring flange width, $V(11) = W(RNG)$, is less than ring spacing, $V(8) = B(RNG)$)
1. $-V(1)^{+1} + 5.V(8)^{-1} - 1$. (stringer spacing, $V(1) = B(STR)$, is less than 5 x ring spacing, $V(8) = B(RNG)$)

Linking constraint:

There is one linking constraint: the stringer base width, $B2(STR)$, must equal 0.1 x (stringer spacing $B(STR)$). In this paper the stringer base has the same thickness and properties as the skin between stringers; there are no faying flanges in any of the cases explored here.

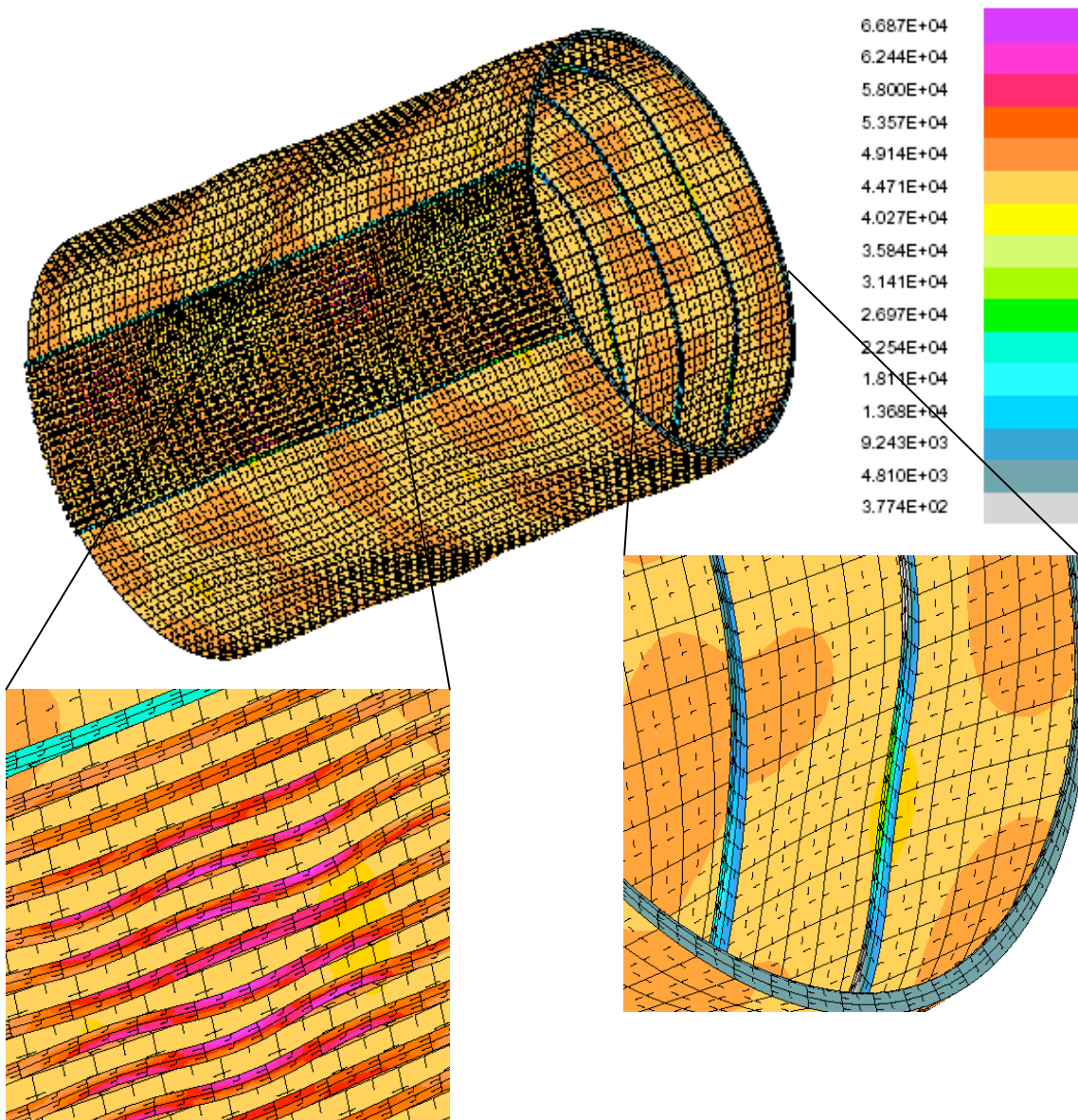
Table 2 Definitions of variables used in the PANDA2 examples

Variable Number	Variable Name	Definition	Structural Part
1	B(STR)	stiffener spacing, b: STR	stringer
2	B2(STR)	width of stringer base, b2 (must be > 0)	stringer
3	H(STR)	height of stiffener (type H for sketch), h	stringer
4	W(STR)	width of outstanding flange of stiffener, w	stringer
5	T(1)(SKN)	thickness for layer index no.(1): SKN seg=1	panel skin
6	T(2)(STR)	thickness for layer index no.(2): STR seg=3	stringer web
7	T(3)(STR)	thickness for layer index no.(3): STR seg=4	stringer flange
8	B(RNG)	stiffener spacing, b: RNG	ring
9	B2(RNG)	width of ring base, b2 (zero is allowed)	ring
10	H(RNG)	height of stiffener (type H for sketch), h	ring
11	W(RNG)	width of outstanding flange of stiffener, w	ring
12	T(4)(RNG)	thickness for layer index no.(4):RNG seg=3	ring web
13	T(5)(RNG)	thickness for layer index no.(5):RNG seg=4	ring flange

Table 4 Optimum designs from PANDA2 suitable for analysis by STAGS (dimensions in inches)

	Case 1 Perfect, no Koiter, ICONSV=1	Case 2 Imperfect, no Koiter, yes change imperfection amplitude, ICONSV=-1	Case 3 Imperfect, no Koiter, yes change imperfection amplitude, ICONSV=0	Case 4 Imperfect, no Koiter, yes change imperfection amplitude, ICONSV=1	Case 5 Imperfect, yes Koiter, yes change imperfection amplitude, ICONSV=1	Case 6 As if perfect, no Koiter, Nx=-6000, sbar=120 ksi ICONSV=1	Case 7 Imperfect, no Koiter, no change in imperfection amplitude, ICONSV=1
Variable Name	Optimum Design	Optimum Design	Optimum Design	Optimum Design	Optimum Design	Optimum Design	Optimum Design
B(STR)	0.75519	0.93500	0.93500	0.98170	0.93500	0.93500	1.5708
B2(STR)	0.075519	0.093500	0.093500	0.0981710	0.093500	0.093500	0.15708
H(STR)	0.39795	0.57079	0.58395	0.63651	0.55261	0.55330	0.92254
W(STR)	0.35593	0.38639	0.36056	0.39946	0.29593	0.36761	0.64833
T(1)(SKN)	0.030240	0.033988	0.033795	0.034878	0.039964	0.044110	0.048160
T(2)(STR)	0.019897	0.028540	0.029197	0.031826	0.027631	0.033536	0.046127
T(3)(STR)	0.022209	0.026779	0.029411	0.022835	0.032576	0.024673	0.033702
B(RNG)	6.25	9.3750	8.3333	8.3333	9.3750	8.3333	15.000
B2(RNG)	0.0	0.0	0.0	0.0	0.0	0.0	0.0
H(RNG)	0.52160	0.79425	0.75877	0.79978	0.77659	0.92137	0.86341
W(RNG)	0.17891	0.10000	0.12313	0.24075	0.31922	0.35255	1.0804
T(4)(RNG)	0.026080	0.039713	0.037939	0.040078	0.038830	0.046069	0.043170
T(5)(RNG)	0.021847	0.097842	0.086763	0.029339	0.037873	0.017627	0.054020
WEIGHT	31.81 lb	39.40 lb	40.12 lb	40.94 lb	41.89 lb	46.83 lb	56.28 lb

Critical margins from PANDA2, Table 5	1, 6a,b, 23a,b, 26, 44, 55, 56, 57, see Table 10	1, 3, 6a,c,e, 10, 23a, 26, 47, 55, 56, 57, see Table 6.	1, 3, 6a,c,e, 10, 23a, 26, 47, 55, 56, 57	1, 3, 6a,c,e, 10, 23a,e, 25, 26, 44, 47, 55, 56, 57	1, 3, 6a,d, 10, 11, 23a, 44, 47, 55, 56, 57	1, 3, 6a,c,e, 10, 11, 23a, 25, 26, 44, 47, 55, 56, 57, 58	1, 3, 6a,c,e, 10, 11, 23e, 25, 26, 44, 46, 55, 56, 57, 58
Almost critical margins from STAGS and mode of elastic collapse	1, 6a, 44, Collapse was not computed	1, 6a, 47, Stringer sideways and first bay collapse at PA=1.04	1, 6a, 47, Stringer sideways and first bay collapse at PA= 1.05	1, 6a, 47, Stringer sideways and first bay collapse at PA=1.08	1, 6a, 47, Stringer sideways and first bay collapse at PA=1.13	1, 6a, 11, 44, 47, Axisymmetric edge collapse at PA=0.970; rv(edge)=0 on 2 curved edges.	1, 6a, 11, 47, Stringer sideways, first,middle and last bay collapse at PA= 1.22(-) PA= 1.15(+)
Tables & Figures pertaining to the case	Table 10, Figs. 3, 33-41	Figs. 8–32		Figs. 1a-c, 2, 4-7, 42-65	Table11, Figs. 66-71	Figs. 72-74	Figs. 75-80
Comments	This shell is not practical because no one can fabricate a perfect structure.	With this option you MUST check the results via a general-purpose code such as STAGS.	With this option you are strongly URGED to check result with use of a general-purpose program.	This option may lead to shells with local skin & stringer bending & therefore possibly excessive stresses.	This is the best option if you do not plan to check PANDA2 designs. Even so, you SHOULD check them.	This widely used option generates a heavy shell. PANDA2 cannot predict axisymmetric collapse.	This option is too conservative, in my opinion. The imperfection can probably be detected easily.



Case 4, Table 4: no Koiter, yes change imperfection, ICONSV=1; also see Figs. 61-63. Nonlinear equilibrium state from STAGS at the load factor, PA=1.00516. The imperfect shell has two initial buckling modal imperfection shapes: Fig. 1a with amplitude, Wimp1=+0.0625 and Fig. 61 with amplitude, Wimp2= -0.0005 inch. Prebuckling bending of the imperfect shell causes redistribution of stresses among the shell skin and the stiffener segments. Also, prebuckling bending gives rise to “flattened” regions with an “effective” circumferential radius of curvature that causes early general buckling. (See the right-most expanded insert).

FIG. 2 Outer fiber effective stress (psi) at axial load, $N_x = -3000 \times 1.00516$ lb/in.

□ WEIGHT OF THE ENTIRE PANEL: 180 degrees of the circumference of the cylindrical shell

"Global" optimization of the perfect shell, Case 1 of Table 4

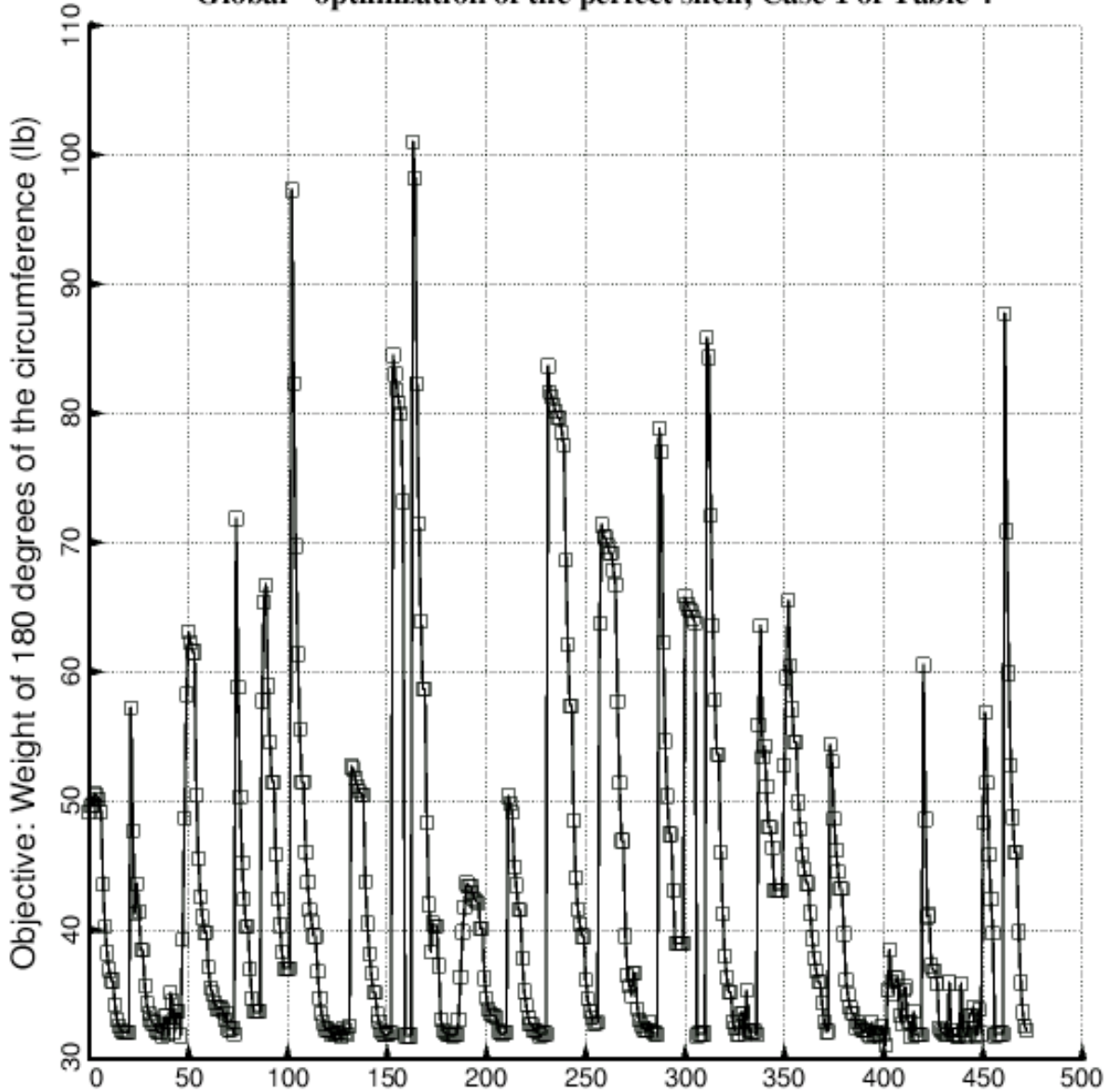
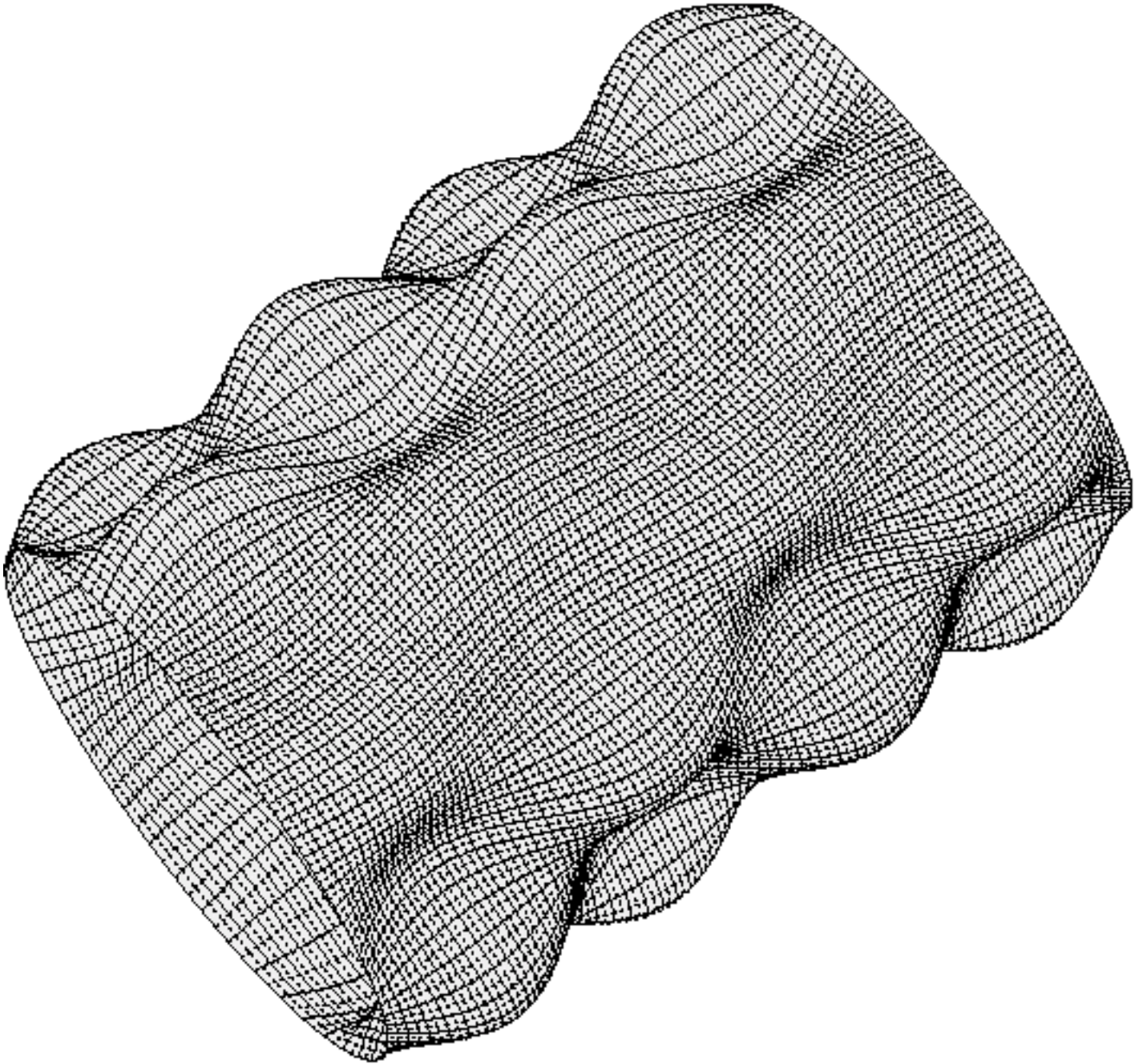


FIG. 3 Design iterations during the first SUPEROPT: Case 1, Table 4

FIG. 3 PANDA2 results for Case 1 in Table 4: Design iterations during an execution of SUPEROPT, a PANDA2 processor the purpose of which is to seek a “global” optimum design. Each “spike” in the plot corresponds to a new starting design, which (as explained in [1D, 1K]) is generated randomly in a manner consistent with all linking and inequality constraints. See Table 3 for a typical PANDA2 runstream that includes several executions of SUPEROPT.



Case 2, Table 4 no Koiter, yes change imperfection, ICONSV= -1. Compare with Fig. 17. STAGS Mode no. 1, load factor, $p_{cr}=1.9189$; PANDA2 predicts 1.890. The linear buckling mode agrees with that from PANDA2: $(m,n)=(4,6)$ halfwaves over 180 deg. See Part 1, Run 1 of Table 9.

FIG. 16 Linear general buckling mode from the STAGS model with all stiffeners smeared.

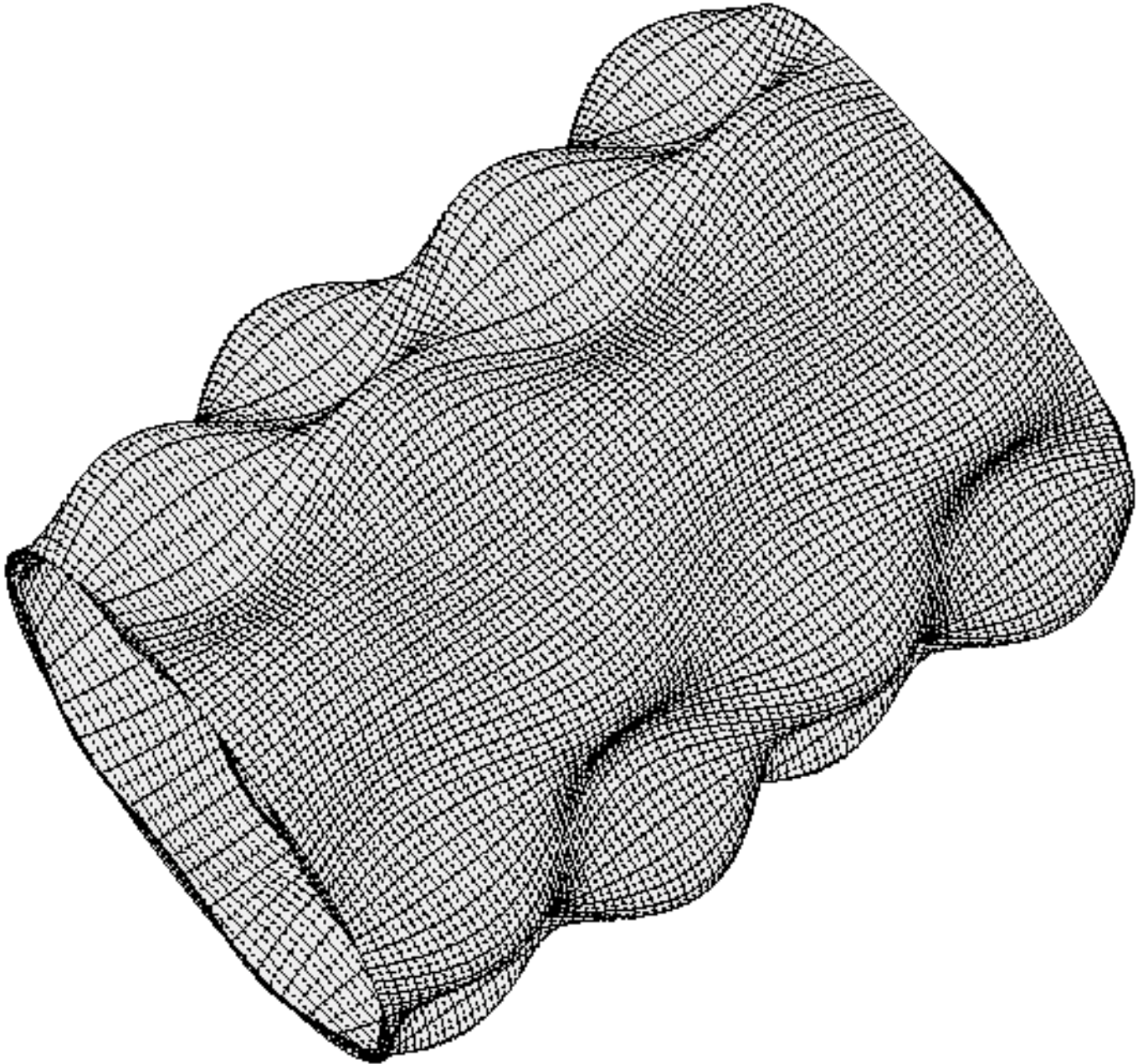


FIG. 17 Linear general buckling mode from the STAGS model. Only the stringers are smeared. The rings are modeled as shell units, 2 shell units per ring: Shell unit (a) for the ring web and Shell unit (b) for the ring outstanding flange. Case 2, Table 4: no Koiter, yes change imperfection, ICONSV = -1; Compare with Fig. 16. STAGS Mode no. 1, load factor, pcr=1.9017; PANDA2 predicts 1.890. The linear buckling mode agrees with that from PANDA2: (m,n)=(4,6) halfwaves over 180 deg. See Part 1, Run 2 in Table 9. This STAGS model and the model in the previous figure are used to obtain good approximations of the general buckling mode shape and load factor (eigenvalue) for two reasons: 1. Determine what circumferential sector to use for more refined models (60 degrees is good in this case), and 2. obtain a good estimate of the initial eigenvalue “shift” to use in the more refined models.

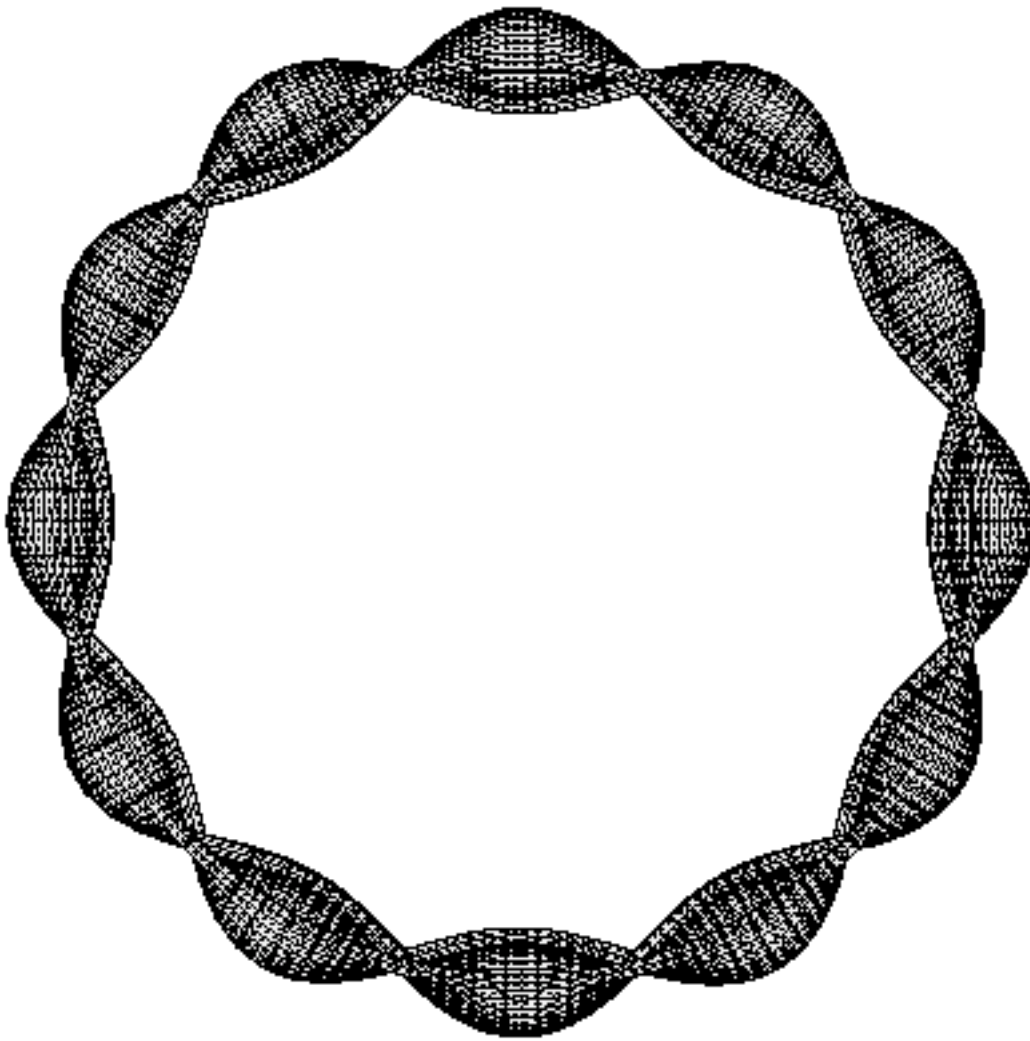


Fig. 18 The same buckling mode from STAGS as that displayed in the previous figure, viewed end-on. One can see that there are 12 half-waves around the circumference, that is, 6 full circumferential waves. (From: AIAA 48th Structures, Structural Dynamics, and Materials Conference, Paper no. AIAA-2007-2216, 2007)

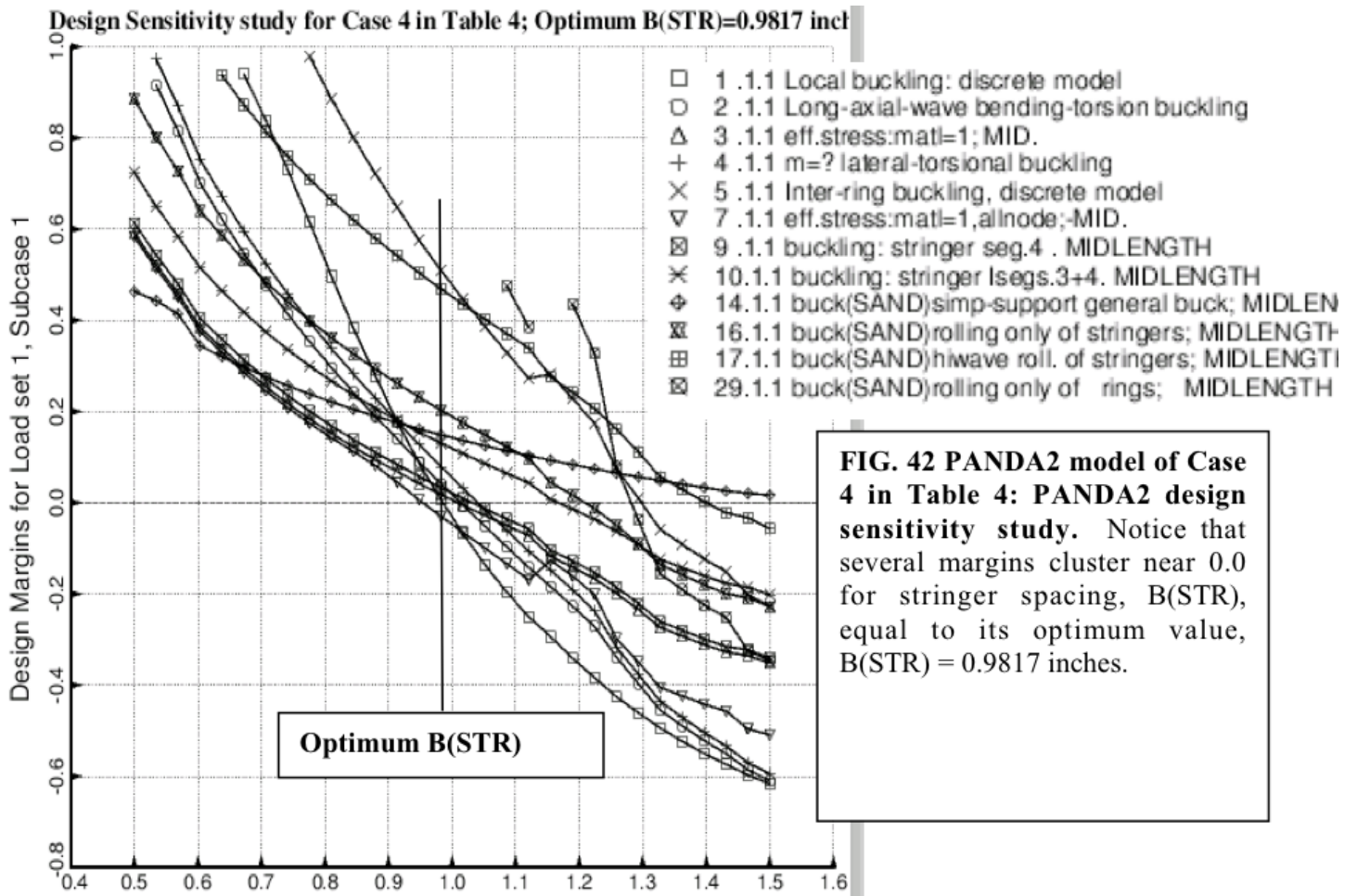


Fig. 42 PANDA2 design sensitivity study: Design Parameter, B(STR) (inches). B(STR) is the stringer spacing. (From: AIAA 48th Structures, Structural Dynamics, and Materials Conference, Paper no. AIAA-2007-2216, 2007)